Aggregation of Copper(II) Tetrasulfonated Phthalocyanine in Aqueous Salt Solutions

Philip J. Camp,* Anita C. Jones, Robert K. Neely, and Neil M. Speirs

School of Chemistry, University of Edinburgh, West Mains Road, Edinburgh EH9 3JJ, United Kingdom

Received: July 17, 2002; In Final Form: September 2, 2002

The aggregation of a copper(II) tetrasulfonated phthalocyanine ($CuPcS_4$) dye in aqueous sodium chloride solution has been studied using UV−vis spectroscopy and statistical mechanics. The concentration dependences of the molar absorption coefficients at 626 and 665 nm have been measured for $CuPcS_4$ solutions with concentrations in the range 10^{-7} to 10^{-3} M and salt concentrations between 0 and 2 M. It is commonly believed that such results can be fitted adequately by assuming that a monomer−dimer equilibrium operates in the solution, but it is shown that this model has serious deficiencies, particularly at low salt concentrations. The experimental results have been analyzed using new expressions derived using statistical mechanics, taking into account the formation of trimers and higher aggregates. The model is based on the fact that $\pi-\pi$ interactions between the essentially planar phthalocyanine molecules favor the formation of columnar aggregates. Therefore, cluster partition functions can be approximated in terms of two parameters corresponding to molecules with one and two nearest neighbors within the stack. The resulting theoretical expressions are shown to provide excellent fits to the experimental results over the entire range of dye and salt concentrations considered. The fitted equilibrium constants using the monomer−dimer equilibrium indicate an increase in aggregation with increasing salt concentration. In contrast, the fitted equilibrium constants from the new theory indicate that aggregation is suppressed at high salt concentrations.

1. Introduction

The aggregation of phthalocyanine (Pc), and related dye molecules, has been the subject of intensive study over many decades.[1] Water-soluble Pcs are used widely as textile dyes, and aggregation has significant effects on the light fastness and color quality of the dyestuff. In recent years, interest in Pc aggregation has been stimulated by the adoption of Pcs as photosensitizers in photodynamic cancer therapy and the observation that aggregates are much less active than monomers. Pcs are usually quite strongly aggregating because the planar molecular geometry admits significant $\pi-\pi$ interactions between molecules, hence stabilizing columnar aggregates. Spectroscopic techniques can often be employed to analyze the nature and degree of aggregation. In Pcs, the UV−vis absorption spectrum is dominated by the Q-band arising from $\pi-\pi^*$ transitions. Usually, one can assign individual peaks within the Q-band to either free molecules or molecules contained within aggregates, and hence the degree of aggregation within the solution can be inferred from the respective peak intensities. In general, the aggregate peak is blue-shifted with respect to the monomer peak because of the cooperative interaction between transition dipole moments on molecules within an aggregate. Quantitative predictions for the shift can be obtained using the molecular exciton approximation.[2] In Pc aggregates, this approximation is compromised by the presence of the strong $\pi-\pi$ interactions, but the general trends remain valid.[3]

One of the earliest systematic studies of Pc aggregation was carried out by Gruen.[4] In this work, the aggregation in two different copper phthalocyanine reactive dyes was investigated by measuring the absorption spectra in various solvents. Spectra measured in aqueous solutions with dye concentrations in the range 2.0×10^{-6} to 2.0×10^{-4} kg L^{-1} showed relatively little variation, which was interpreted as indicating a very high equilibrium constant, such that the dye was almost entirely associated over this concentration range. Spectra measured at fixed solute concentration (2.0×10^{-6} kg L^{-1}) in different solvents, or at different ionic strengths, were observed to intersect at isosbestic points, suggesting that a simple monomer−dimer equilibrium operates in these systems. On the basis of the relative monomer and aggregate peak heights, it was concluded that aggregation increases with increasing solvent polarity and with increasing salt concentration. These results were explained on the basis of ionic and dielectric screening of the repulsions between like charges on the solvated Pc molecules.

There have been many subsequent studies of aggregation in solutions of phthalocyanine compounds (e.g., refs 3, 5, and 6). In ref 5, Yang et al. studied the monomer−dimer equilibrium in cobalt tetrasulfonated phthalocyanines in water and aqueous alcoholic solutions with solute concentrations up to 2×10^{-5} M. Equilibrium constants extracted from absorption measurements indicated nontrivial solvent effects that were probably due to the interplay between solute−solvent and water−alcohol interactions.

In ref 6, Martin et al. investigated the effects of pH and ionic strength on the dimerization of aluminum and zinc sulfonated phthalocyanines in aqueous solution, with solute concentrations up to 10^{-5} M. It was concluded that an increase in pH or ionic strength leads to an increase in the monomer−dimer equilibrium constant.

In ref 3, Schutte et al. investigated the aggregation of a metal-free octasubstituted Pc in dodecane solution over Pc concentrations in the range $10^{-7}$to 10^{-2} M. UV−vis absorption spectra at different Pc concentrations were analyzed on the assumption that each spectrum is a superposition of individual monomer and aggregate spectra, weighted by the respective mole fractions. Results over the entire concentration were analyzed on the basis of a monomer−dimer equilibrium and over a restricted range up to 5×10^{-4} M assuming a monomer−dimer−trimer equilibrium. The monomer−dimer equilibrium constant was found to be on the order of 10^6, whereas that for the dimer−

10.1021/jp026551o CCC: $22.00
Published on Web 10/08/2002

trimer equilibrium was around 2 orders of magnitude smaller. Discrepancies between the fitted spectra and the experimental results became significant at only the highest concentrations and were attributed not only to the presence of tetramers and higher aggregates but also to the onset of discotic liquid-crystalline ordering of the aggregates.[7−9] This occurs at quite low Pc concentrations because the octasubstituted Pc is so bulky, which increases the entropic driving force for the development of orientational order. In ref 3, Schutte et al. observed that the aggregation of octasubstituted Pc is pronounced in low-polarity solvents such as dodecane, which has a dielectric constant of $\epsilon = 2.0$. This was attributed to the screening of the intermolecular interactions responsible for aggregation being minimized in such media. On this basis, an increase in solvent polarity should be accompanied by a decrease in solute aggregation, in contradiction with the claims of ref 4.

Studies of dye aggregation have not been limited to phthalocyanine compounds. Recently, Neumann and co-workers studied the aggregation of an azo dye, Acid Red 266, in aqueous solution by means of UV−vis spectroscopy, nuclear magnetic resonance spectroscopy, and static light scattering.[10,11] In these studies, dye concentrations were less than 5×10^{-6} M, and in ref 10, it was shown that a simple monomer−dimer equilibrium is sufficient to describe the observed concentration dependence of the absorption spectra. The effects of adding salt to the dye solution were also investigated in this study, the conclusion being that equilibrium constants increase with increasing salt concentration, in agreement with the general trends observed in refs 4 and 6. In ref 11, an equilibrium model that includes the contribution of higher aggregates was also tested. In this model, it is assumed that all of the relevant equilibrium constants are equal, which, if anything, should lead to an overestimation of the concentrations of trimers and higher aggregates. As we will show below, the predictions of a theory that contains only one distinct equilibrium constant will not be qualitatively very different from those based on the simple monomer−dimer equilibrium.

The consensus appears to be that the aggregation of phthalocyanine and azo dyes is well described by a simple monomer−dimer equilibrium and that an increase in ionic strength or solvent polarity increases the corresponding equilibrium constant. Perhaps the only counterevidence put forward to date is that presented by Schutte et al.[3] This work is distinguished by the wide range of dye concentrations considered and by the fact that the formation of trimers was shown to be significant even at quite low concentrations ($c > 10^{-4}$ M).

To investigate the high solute-concentration regime further, we have studied a copper(II) tetrasulfonated phthalocyanine ($CuPcS_4$) dye in aqueous solutions, with and without added salt, using UV−vis spectroscopy. The $CuPcS_4$ studied is an example of a commercial reactive textile dye and carries a monochlorotriazine substituent that is the reactive group that binds the dye to the textile fiber. The $CuPcS_4$ concentrations considered in this work are in the range $10^{-7} \le c \le 10^{-3}$ M. As in previous studies, the nature and extent of aggregation was inferred by monitoring molar absorption coefficients as functions of dye concentration. We will show that the simple monomer−dimer equilibrium and an unlimited-aggregation theory similar to that proposed in ref 11 provide poor descriptions of the aggregation in $CuPcS_4$ solutions with little or no added salt by virtue of having only one fitted equilibrium constant. It would therefore appear that aggregation may not be limited to the formation of dimers or trimers and that proper account should be taken of the presence of higher aggregates. It is likely that the clusters consist of columns of the roughly planar $CuPcS_4$ molecules, and a theory has been developed for the full equilibrium distribution of clusters formed by such stacks of molecules, ranging from monomers to stacks with infinite extent. The predicted equilibrium cluster distribution is characterized by two parameters. In molecular terms, these parameters reflect the different degrees of confinement experienced by molecules at the ends of a cluster, having one nearest neighbor, and those in the middle of the cluster, having two nearest neighbors. Fits of these new expressions to the experimental results show excellent agreement.

In accord with earlier studies,[4,10] a naïve analysis of our experimental results using the monomer−dimer equilibrium suggests that the equilibrium constant increases with salt concentration. By contrast, an analysis using the new and quantitatively correct model shows that at low salt concentrations (~0.01 M) aggregation is enhanced slightly with respect to the pure-water solution, whereas at higher salt concentrations, aggregation is actually suppressed. At the highest salt concentrations (0.1 and 2 M), the new theory and the theories containing only one equilibrium constant converge, indicating that the mole fractions of molecules in trimers and higher aggregates can be safely ignored.

This paper is organized as follows. In section 2, we summarize the experimental methods employed in this work. Expressions for the equilibrium cluster distribution are derived in section 3. The results are presented in section 4, and section 5 concludes the paper.

2. Experimental Section

The $CuPcS_4$ was a gift from DyStar UK Ltd. The supplier estimated that the material consists of >95% tetrasulfonated phthalocyanine species, with the sulfonate groups located predominantly at the 4 (β) positions, as opposed to the 3 (α) positions. Sample solutions were prepared by dilution from a stock solution of 1.0×10^{-3} M $CuPcS_4$ in deionized water using an Eppendorf "Reference" micropipet (100−1000 μL) and volumetric flasks. To minimize cumulative dilution errors, no more than two successive dilutions were used to prepare any one solution. Absorbance measurements were made on a Unicam model UV-2 double-beam UV−vis spectrometer using a spectral band-pass of 2 nm and a signal integration time of 2 s. Matched pairs of glass cuvettes with the following path lengths, l, were used: 100 mm for 1.0×10^{-7} M $\le c \le 5.0 \times 10^{-6}$ M; 10 mm for 1.0×10^{-5} M $\le c \le 5.0 \times 10^{-5}$ M; and 1 mm for 1.0×10^{-4} M $\le c \le 1.0 \times 10^{-3}$ M. The absorbance, A, was measured at two wavelengths, 626 and 665 nm, taking the average of five measurements for each sample at each wavelength. From measurements on multiple samples prepared at the same concentration, it was estimated that the relative statistical uncertainties in the measured values of the absorbance were less than 1.5%. Results are reported in terms of the molar absorption coefficient, $\epsilon = A/cl$.

3. Theory

3.1. Equilibrium Distribution of Aggregates. In this section, we derive expressions for the equilibrium distribution of stack-like clusters, using statistical mechanics. We shall see that the results are equivalent to those that would be obtained from thermodynamics alone by assuming a priori only two distinct equilibrium constants—one for the monomer−dimer equilibrium and the other for successive inclusions of additional monomers. The statistical mechanics approach, however, yields a clear interpretation of the relative magnitudes of the two constants.

The derivation below is along similar lines to that used by van Roij in studies of aggregation and phase transitions in strongly interacting dipolar fluids.[12,13]

Consider a solution containing N solute molecules in a volume V and at a temperature T. At equilibrium, there are N_1 free monomers, N_2 dimers, and in general N_n n-mers. The corresponding concentration of n-mers is given by $c_n = N_n/V$. The total concentration of monomers, $c = N/V$, is related to the values of c_n by

$$c = \sum_{n=1}^{\infty} n c_n \tag{1}$$

The conditions for thermodynamic equilibrium are

$$\mu_n = n\mu_1 \qquad (n \geq 1) \tag{2}$$

where μ_n is the chemical potential of n-mers. The cluster concentrations considered in this work are sufficiently low ($c \leq 10^{-3}$ M) that interactions between the clusters can be ignored, and so the solution is considered ideal. In a solution of noninteracting clusters, the partition function for the solution (ignoring the solvent degrees of freedom) is

$$Q = \prod_{n=1}^{\infty} \frac{q_n^{N_n}}{N_n!} \tag{3}$$

where q_n is the partition function of an n-mer. In eq 3, we have assumed that aggregates of a particular size are indistinguishable (i.e., there are no stereoisomers). We shall further assume that an n-mer ($n \geq 2$) is formed from a "stack" of monomers and thus contains two "external" molecules with one nearest neighbor and ($n - 2$) "internal" molecules with two nearest neighbors. From these considerations, we write q_n in the form

$$q_1 = \frac{V}{\Lambda^3} \tag{4}$$

$$q_n = \frac{V \upsilon_{ex} \upsilon_{in}^{n-2}}{\Lambda^{3n}} \qquad (n \geq 2) \tag{5}$$

where Λ is the de Broglie thermal wavelength of a single molecule, V is the volume accessible to the first external molecule in the stack, and υ_{ex} and υ_{in} are single-molecule parameters, with units of volume, that reflect how rigidly an external or internal molecule is constrained by its neighbor(s). We anticipate that $\upsilon_{ex} > \upsilon_{in}$ because an external molecule with only one nearest neighbor should be less strongly constrained than an internal molecule, which has two nearest neighbors. Roughly speaking, υ_{ex} and υ_{in} will also contain factors proportional to $\exp(-E/k_BT)$, where k_B is Boltzmann's constant and E is the energy "per bond". The partition function (eq 3) is related to the Helmholtz free energy, F, and the chemical potentials, μ_n, by the fundamental equations $F = -k_BT \ln Q$ and $\mu_n = (\partial F/\partial N_n)$, from which we obtain

$$\mu_1 = k_BT \ln(c_1 \Lambda^3) \tag{6}$$

$$\mu_n = k_BT \ln\left(\frac{c_n \Lambda^{3n}}{\upsilon_{ex} \upsilon_{in}^{n-2}}\right) \tag{7}$$

By inserting eqs 6 and 7 into eq 2, we arrive at the following relation between c_1 and c_n ($n \geq 2$):

$$c_n = \upsilon_{ex} \upsilon_{in}^{n-2} c_1^n \tag{8}$$

Using eq 8, it is easy to show that the equilibrium constant governing the equilibrium (monomer + monomer $\rightleftharpoons$ dimer) is equal to υ_{ex} and that the equilibrium constant governing the equilibrium (n-mer + monomer $\rightleftharpoons$ $\{n + 1\}$-mer ($n \geq 2$)) is equal to υ_{in}. It is important to recognize that, in general, all such equilibria can have distinct equilibrium constants. In the present case, where molecules can stack up to form columns, it is reasonable to expect that simply distinguishing υ_{ex} from υ_{in} will provide an adequate description.

Strictly speaking, eqs 6 and 7 and all subsequent relations should contain activity coefficients that take into account solute−solute and solute−solvent interactions. The dominant interactions are likely be Coulombic in nature, particularly in the presence of added salt. However, we do not yet know the oxidation states of the free molecules or the clusters in solution, so it is hard to estimate the activity coefficients even at the Debye−Hückel level. Nonetheless, general trends in the relative stabilities of monomers and clusters should be evident in the values of υ_{ex} and υ_{in} obtained by assuming an ideal solution.

Inserting eq 8 for c_n into eq 1 and summing the resulting geometric series leads to the following equation for c_1:

$$c = c_1 + \frac{\upsilon_{ex} c_1^2 (2 - \upsilon_{in} c_1)}{(1 - \upsilon_{in} c_1)^2} \tag{9}$$

To analyze the effective molar absorption coefficients measured experimentally requires predictions for the mole fractions of molecules in different environments, $x_1 = c_1/c$, etc. Using the fact that there are two external molecules per cluster and making use of eq 8 for c_n, we arrive at the following results for x_1, x_{ex}, and x_{in}:

$$1 = x_1 + \frac{\upsilon_{ex} c x_1^2 (2 - \upsilon_{in} c x_1)}{(1 - \upsilon_{in} c x_1)^2} \tag{10}$$

$$x_{ex} = 2 \sum_{n=2}^{\infty} \frac{c_n}{c} = \frac{2\upsilon_{ex} c x_1^2}{(1 - \upsilon_{in} c x_1)} \tag{11}$$

$$x_{in} = 1 - x_1 - x_{ex} > 0 \tag{12}$$

This model will be referred to as UA1 (unlimited aggregation, model 1). To extract an explicit expression for x_1 from eq 10 requires solving a cubic equation; for reference, this is detailed in the Appendix.

We note two limiting cases of model UA1. When $\upsilon_{in} = \upsilon_{ex}$, there is just one equilibrium constant governing all equilibria of the type monomer + n-mer $\rightleftharpoons$ $\{n + 1\}$-mer, including the monomer−dimer equilibrium. The composition of the solution is then given by

$$x_1 = \frac{1}{\upsilon_{ex} c} + \frac{(1 - \sqrt{1 + 4\upsilon_{ex} c})}{2(\upsilon_{ex} c)^2} \tag{13}$$

$$x_{ex} = \frac{2\upsilon_{ex} c x_1^2}{(1 - \upsilon_{ex} c x_1)} \tag{14}$$

$$x_{in} = 1 - x_1 - x_{ex} > 0 \tag{15}$$

We will refer to this model as UA2 (unlimited aggregation, model 2).

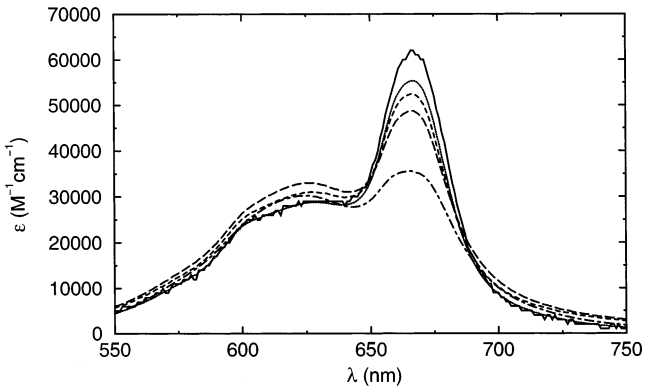

Figure 1. Molar absorption coefficients for $CuPcS_4$ solutions in pure water: $c = 1 \times 10^{-7}$ M (—), $c = 1 \times 10^{-6}$ M (•••), $c = 1 \times 10^{-5}$ M (- - -), $c = 1 \times 10^{-4}$ M (— — —), $c = 1 \times 10^{-3}$ M (• — •).

When $\upsilon_{in} = 0$, solving eqs 10−12 yields the explicit relations

$$x_1 = \frac{-1 + \sqrt{1 + 8\upsilon_{ex}c}}{4\upsilon_{ex}c} \tag{16}$$

$$x_{ex} = 2\upsilon_{ex}cx_1^2 \tag{17}$$

$$x_{in} = 1 - x_1 - x_{ex} = 0 \tag{18}$$

which correspond to the familiar results for a monomer−dimer equilibrium, with the equilibrium constant proportional to υ_{ex}. We will denote this model by MD (monomer−dimer model).

Finally, in an examination of the equilibrium cluster distribution, it is useful to define a cluster fraction, X_n, that is equal to the fraction of clusters that are n-mers:

$$X_1 = \frac{c_1}{\sum_{n=1}^{\infty} c_n} = \frac{x_1}{x_1 + \frac{1}{2}x_{ex}} \tag{19}$$

$$X_n = \frac{c_n}{\sum_{n=1}^{\infty} c_n} = \frac{x_1^n(\upsilon_{ex}c)(\upsilon_{in}c)^{n-2}}{x_1 + \frac{1}{2}x_{ex}} \qquad (n \geq 2) \tag{20}$$

3.2. Molar Absorption Coefficients. In analyzing experimental results, it is assumed that we can assign distinct molar absorption coefficients to single molecules, external molecules, and internal molecules, denoted by $\epsilon_1(\lambda)$, $\epsilon_{ex}(\lambda)$, and $\epsilon_{in}(\lambda)$, respectively. The apparent molar absorption coefficient, $\epsilon(\lambda)$, at a particular wavelength, λ, is therefore equal to

$$\epsilon(\lambda) = x_1\epsilon_1(\lambda) + x_{ex}\epsilon_{ex}(\lambda) + x_{in}\epsilon_{in}(\lambda) \tag{21}$$

The concentration dependence of $\epsilon(\lambda)$ is contained in the variation of x_1, x_{ex}, and x_{in}, as predicted by models UA1, UA2, and MD.

4. Results

In Figure 1 we show absorption spectra in the range 550 nm $\leq \lambda \leq$ 750 nm for pure-water solutions of $CuPcS_4$ with concentrations in the range 10^{-7} to 10^{-3} M. The spectra are typical of those observed for Pc compounds: the narrow longer-wavelength band (at 665 nm) corresponds to the monomer 0−0 transition; the broader band at lower wavelength (626 nm) is attributed to those molecules within aggregates. This is on the basis that the transition dipole moment of a cluster should be greater than that of a monomer, and hence the excitation energy is blue-shifted. Note that the molar absorption coefficient at 665 nm decreases with increasing concentration, signaling an increase in aggregation. The absorption coefficient of the aggregate band is less sensitive to changes in concentration, but roughly speaking, it first rises with increasing dye concentration and then falls at a dye concentration of 10^{-3} M. Note the absence of any isosbestic points, which suggests that the aggregation is not of the simple monomer−dimer type.

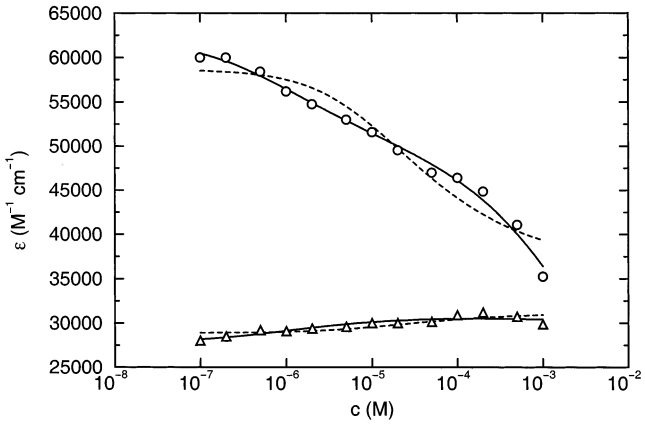

Figure 2. Molar absorption coefficients, ϵ, at $\lambda = 626$ (△) and 665 nm (○) as functions of $CuPcS_4$ concentration in pure water. The curves are fits using models introduced in the text: UA1 (—), and MD (- - -). Note the logarithmic scale on the x axis.

In Figure 2, we show the molar absorption coefficients at 626 and 665 nm as functions of $CuPcS_4$ concentration in pure-water solutions. At 665 nm, there appears to be a point of inflection at $c \simeq 1.0 \times 10^{-6}$ M and a sharp decrease at $c > 10^{-4}$ M. The occurrence of such well-separated features suggests that two types of equilibria are operating in the solution—one at low concentrations, $c \simeq 10^{-6}$ M, and one at higher concentrations, $c \simeq 10^{-4}$ M.

The experimental results were fitted using models UA1, UA2, and MD. In all cases, the parameters υ_{ex} and υ_{in} were determined by fitting to the results at 665 nm because the concentration dependence of ϵ was most pronounced at this wavelength. In this way, the quality of the fit is not compromised by those sections of the molar absorption spectrum that show a very weak concentration dependence. Molar absorption coefficients at wavelengths in the range 550 nm $\leq \lambda \leq$ 750 nm were then fitted using the values of υ_{ex} and υ_{in} determined from the results at 665 nm.

The molar absorption coefficients at 626 and 665 nm of $CuPcS_4$ in pure-water solutions as fitted by models UA1 and MD are shown in Figure 2. The fits using model UA2 are omitted for clarity because on the scale of the Figure they are indistinguishable from those using model MD, although the fit parameters are different. The Figure clearly shows the poor qualitative description provided by model MD (and by extension, model UA2). At 665 nm, model UA1 is clearly superior to models UA2 and MD in that it captures the features at $c > 10^{-4}$ M as well as at the asymptotic low-concentration limit in which $\epsilon \rightarrow \epsilon_1$. The models are comparable at 626 nm because ϵ_1, ϵ_{ex}, and ϵ_{in} are all very similar at this wavelength (see Table 1). We note that even though model UA2 takes into account the possibility of unlimited aggregation the fact that there is only one fitted equilibrium constant restricts the shape of the curve to be almost coincident with the best-fit curve obtained using model MD.

TABLE 1: Fit Parameters from Models UA1, UA2, and MD[a]

solvent (M)	model	υ_{ex}	υ_{in}	$\epsilon_1(626)$	$\epsilon_{ex}(626)$	$\epsilon_{in}(626)$	$\epsilon_1(665)$	$\epsilon_{ex}(665)$	$\epsilon_{in}(665)$
		(M^{-1})				(10^4 M^{-1} cm^{-1})			
water	UA1	6.3×10^5	2.4×10^4	2.79(3)	3.09(3)	2.9(2)	6.2(1)	5.0(1)	~0
	UA2	9.1×10^4	9.1×10^4	2.85(2)	3.13(6)	3.03(4)	5.9(1)	5.1(1)	3.6(3)
	MD	2.8×10^4		2.89(2)	3.12(3)		5.9(1)	3.7(2)	
0.01 M NaCl(aq)	UA1	9.4×10^5	2.6×10^4	2.68(5)	2.98(4)	3.0(3)	5.7(2)	4.5(1)	~0
	UA2	1.5×10^5	1.5×10^5	2.74(4)	3.01(8)	2.95(5)	5.39(1)	4.7(1)	3.4(2)
	MD	4.7×10^4		2.79(3)	3.02(4)		5.4(1)	3.5(1)	
0.1 M NaCl(aq)	UA1	1.5×10^5	7.3×10^3	2.71(5)	3.03(8)	1.7(7)	5.09(6)	3.6(1)	~0
	UA2	1.6×10^5	1.6×10^5	2.68(5)	3.1(1)	2.76(7)	5.01(9)	4.3(1)	3.0(1)
	MD	5.1×10^4		2.77(5)	2.90(6)		5.01(7)	3.00(9)	
2 M NaCl(aq)	UA1	7.8×10^4	1.0×10^2	2.25(9)	2.6(3)	~0	3.73(6)	2.4(6)	~0
	UA2	1.1×10^5	1.1×10^5	2.16(7)	3.0(2)	1.9(3)	3.72(6)	2.8(9)	2.4(4)
	MD	7.8×10^4		2.25(7)	2.6(1)		3.73(4)	2.3(1)	

[a] Figures in parentheses are the estimated statistical uncertainties in the last digits.

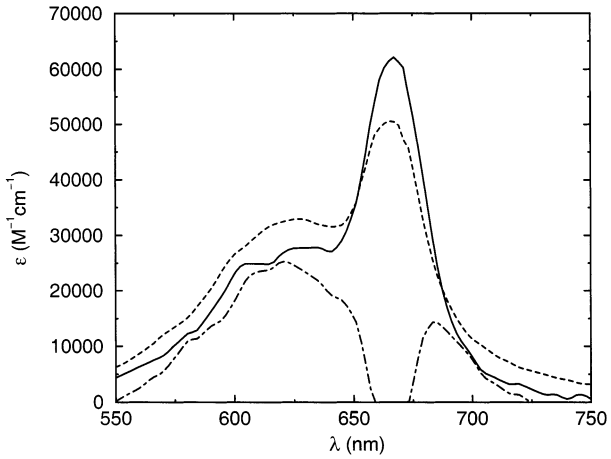

Figure 3. Fitted molar absorption coefficients of monomer, internal, and external molecules of $CuPcS_4$ in pure water using model UA1: $\epsilon_1(\lambda)$ (—), $\epsilon_{ex}(\lambda)$ (- - -), and $\epsilon_{in}(\lambda)$ (• — •).

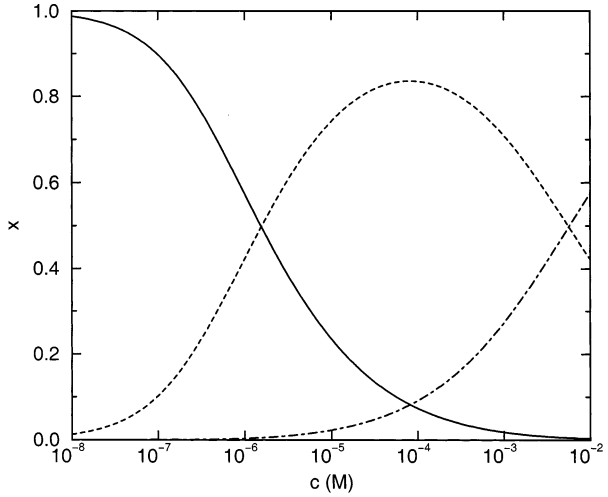

Figure 4. Fractions of molecules of different types as functions of the $CuPcS_4$ concentration in pure water from model UA1: fraction of monomer molecules, x_1 (—); fraction of external molecules, x_{ex} (- - -); and fraction of internal molecules, x_{in} (• — •). Note the logarithmic scale on the x axis.

The fitted equilibrium constants for all models are presented in Table 1 along with the corresponding individual molar absorption coefficients at 626 and 665 nm. Statistical uncertainties are given for ϵ_1, ϵ_{ex}, and ϵ_{in}, and for the most part, the relative errors are less than 10%. Statistical errors in the fit parameters for model UA2 are larger than those for models UA1 and MD largely because of the constraint imposed by having equal values of υ_{ex} and υ_{in} in the former. The relative errors in all estimates of υ_{ex} and υ_{in} are very large, on the order of 100%. This is due to the insensitivity of the various expressions for x_1, x_{ex}, and x_{in} on υ_{ex} and υ_{in}. For this reason, statistical errors for υ_{ex} and υ_{in} have been omitted from Table 1, as it proved impossible to obtain meaningful and reliable estimates. The orders of magnitude should be reliable, however. The UA1 fit parameters for the pure-water solutions indicate that $\upsilon_{ex} \simeq 10^6$ M^{-1} and $\upsilon_{in} \simeq 10^4$ M^{-1}. These figures are in broad agreement with those for the dimer and trimer equilibrium constants obtained by Schutte et al. for an octasubstituted Pc.[3] The MD model gives values of υ_{ex} over an order a magnitude smaller than does model UA1, and model UA2 yields values somewhere in between.

Figure 3 shows the fitted molar absorption coefficients $\epsilon_1(\lambda)$, $\epsilon_{ex}(\lambda)$, and $\epsilon_{in}(\lambda)$ in the range 550 nm $\leq \lambda \leq$ 750 nm using model UA1 with the values of υ_{ex} and υ_{in} determined at 665 nm. The monomer spectrum, $\epsilon_1(\lambda)$, and external-molecule spectrum, $\epsilon_{ex}(\lambda)$, exhibit strong peaks in the region of 665 nm; there seems to be a very slight blue-shifting of this principal peak in $\epsilon_{ex}(\lambda)$ with respect to that in $\epsilon_1(\lambda)$. All three spectra possess broad features at around 626 nm. At first sight, the fitted internal-molecule spectrum, $\epsilon_{in}(\lambda)$, appears very unusual. This can be explained by considering the high-concentration dependence of the molar absorption coefficient in the region of 665 nm. We would expect that at very high $CuPcS_4$ concentrations $\epsilon(\lambda)$ should approach a finite value equal to $\epsilon_{in}(\lambda)$. In Figure 2, however, we see that at the highest concentration accessible in our experiments ($c = 10^{-3}$ M) $\epsilon(665)$ has yet to level off, and hence our ability to fit $\epsilon_{in}(\lambda)$ in the region of 665 nm is severely limited. Nonetheless, it is clear that $\epsilon_{ex}(\lambda)$ and $\epsilon_{in}(\lambda)$ must be considerably different, as shown in Figure 3, particularly at wavelengths in the region of 665 nm.

The variations of the equilibrium cluster distributions with $CuPcS_4$ concentration in pure-water solutions according to model UA1 are illustrated in Figures 4 and 5. Figure 4 shows the mole fraction of molecules in each of the free-monomer, external, and internal environments (eqs 10−12). At low concentrations ($c \simeq 10^{-7}$ M), the molecules are largely unclustered, and hence x_1 is close to unity. At the higher concentrations ($c \simeq 10^{-3}$ M), large clusters are present, and hence a sizable percentage (~30%) of molecules will be accommodated within the bodies of the aggregates. At intermediate concentrations ($c \simeq 10^{-4}$ M), the fraction of external molecules reaches a maximum due to a majority of dimers. This is borne out in Figure 5, which shows the mole fraction of

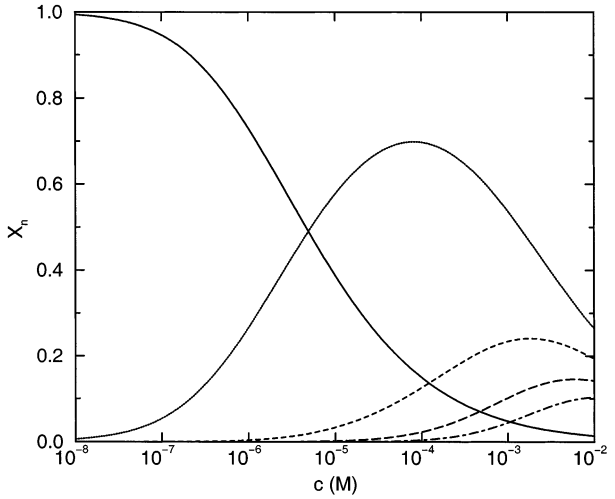

Figure 5. Fractions of aggregates containing *n* molecules as functions of $CuPcS_4$ concentration in pure water from model UA1: X_1 (—), X_2 (···), X_3 (- - -), X_4 (— — —), and X_5 (· — ·). Note the logarithmic scale on the *x* axis.

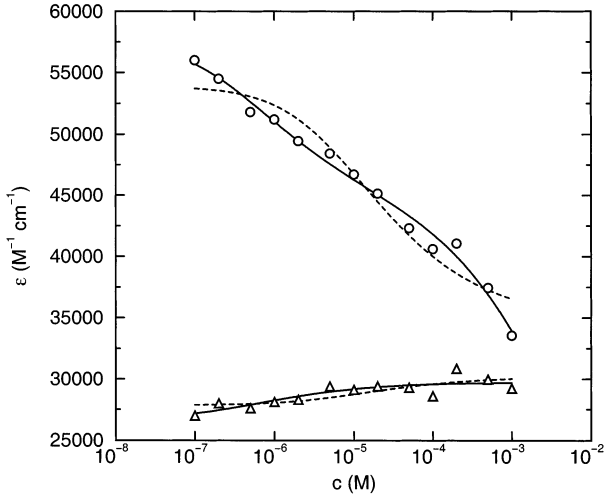

Figure 6. Molar absorption coefficients, ϵ, at $\lambda = 626$ (△) and 665 nm (○) as functions of $CuPcS_4$ concentration in 0.01 M NaCl solution. The curves are fits using models introduced in the text: UA1 (—) and MD (- - -). Note the logarithmic scale on the *x* axis.

n-mers, X_n, as a function of $CuPcS_4$ concentration (eqs 19−21). In accord with the results in Figure 4, the dimer fraction, X_2, reaches a maximum at $c \simeq 10^{-4}$ M. The mole fractions of the higher clusters exhibit maxima at successively higher concentrations.

The molar absorption coefficients of $CuPcS_4$ at 626 and 665 nm in 0.01 M NaCl solutions are shown in Figure 6. The equilibrium constants were obtained by fitting the concentration dependence of the molar absorption coefficient at 665 nm. The fits using model UA2 are omitted for clarity because on the scale of the Figure they are indistinguishable from those using model MD, although the fit parameters are different. At 665 nm, the fits provided by model UA1 are superior to those provided by model MD, once again illustrating the significance of trimers and higher aggregates. As for the pure-water solution, the three models provide similar-quality fits at 626 nm. The corresponding fit parameters are presented in Table 1. All three models yield increased values for the equilibrium constants up to about 70% larger than the corresponding values in pure-water solution. It should be remembered that the relative statistical uncertainties in υ_{ex} and υ_{in} are likely to be on the order of 100%, so it is unclear whether these deviations are statistically

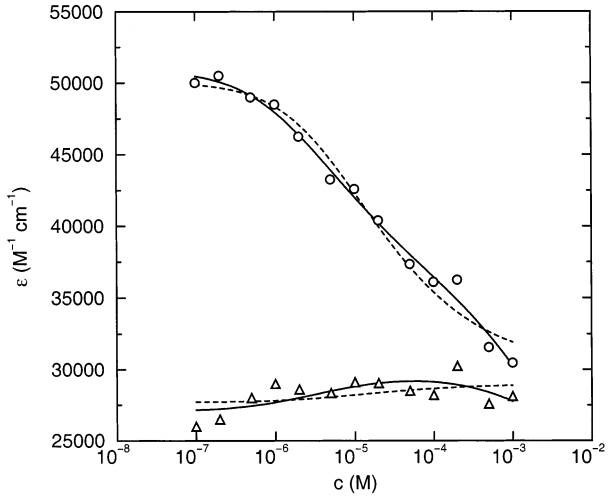

Figure 7. Molar absorption coefficients, ϵ, at $\lambda = 626$ (△) and 665 nm (○) as functions of $CuPcS_4$ concentration in 0.1 M NaCl solution. The curves are fits using models introduced in the text: UA1 (—) and MD (- - -). Note the logarithmic scale on the *x* axis.

significant. However, the fitted values for all three models have increased, which suggests a systematic increase in the degree of aggregation with increasing salt concentration, so far in accord with earlier studies.[4,6,10]

The molar absorption coefficients of $CuPcS_4$ at 626 and 665 nm in 0.1 M NaCl solutions are shown in Figure 7. The equilibrium constants were obtained by fitting the concentration dependence of the molar absorption coefficient at 665 nm. The fits using model UA2 are omitted for clarity because on the scale of the Figure they are indistinguishable from those using model MD, although the fit parameters are different. Interestingly, the fits using model UA1 are quite close to those using the MD model. There is no longer a pronounced high-concentration feature in $\epsilon(665)$, and the fact that the MD model provides a fit that is at least qualitatively acceptable indicates that the contributions of trimers and higher aggregates are less significant in 0.1 M NaCl solution than they are at lower salt concentrations. The implication, therefore, is that the degree of aggregation is suppressed relative to that in the absence of salt. Quantitative evidence for the suppression of aggregation can be found in the fit parameters presented in Table 1. Using model UA1, the values of both υ_{ex} and υ_{in} are significantly smaller than those found in the absence of salt. By contrast, the MD model predicts an increased equilibrium constant, in keeping with earlier studies.[4,6,10]

Molar absorption coefficients of $CuPcS_4$ at 626 and 665 nm in a 2 M NaCl solution are shown in Figure 8. The equilibrium constants were obtained by fitting the concentration dependence of the molar absorption coefficient at 665 nm. The fits using model UA2 are omitted for clarity because on the scale of the Figure they are indistinguishable from those using model MD, although the fit parameters are different. At this very high salt concentration, the three models have provided fits that collapse onto a single curve, indicating that the contribution of trimers and higher aggregates is completely insignificant over the range of $CuPcS_4$ concentrations considered. The fit parameters in Table 1 confirm that the fitted values of υ_{ex}, ϵ_1, ϵ_{ex}, and ϵ_{in} using models UA1 and MD agree very closely. The fitted value of υ_{in} using model UA1 is only $\sim$10 M^{-1}, which is insignificant over the range of $CuPcS_4$ concentrations considered in this work. The value of υ_{ex} from model UA2 is at odds with those from models UA1 and MD because of the inclusion of trimers of higher aggregates.

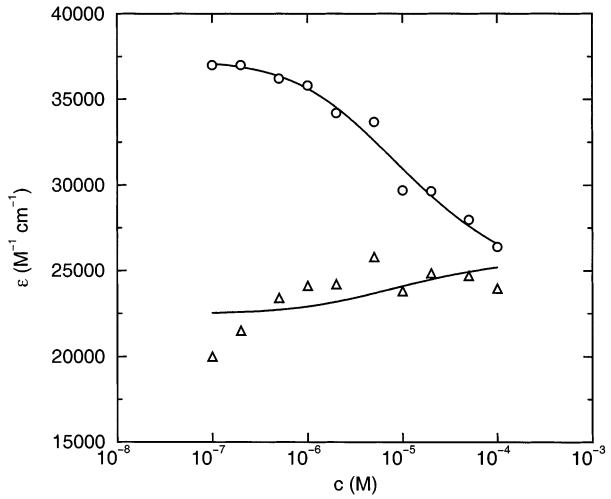

Figure 8. Molar absorption coefficients, ϵ, at $\lambda = 626$ (△) and 665 nm (○) as functions of $CuPcS_4$ concentration in 2 M NaCl solution. The curves are fits using models introduced in the text: UA1 (—) and MD (- - -). Note the logarithmic scale on the *x* axis and that the UA1 and MD curves are coincident.

The fitted molar absorption coefficients at both 626 and 665 nm from all of the models show a downward trend as the salt concentration is increased. This can be understood by appealing to the theory of Myers and Birge.[14] By considering the effect of the coupling between the transition dipole moments on solute and solvent molecules, one may predict the oscillator strength, *f*, of a solute molecule in a solvent with refractive index *n* to be proportional to

$$f \propto 1 - 3G\left(\frac{n^2 - 1}{n^2 + 2}\right) \tag{22}$$

where the factor *G* depends on the geometry of the molecule and on the orientation of the transition dipole moment with respect to the molecular axes. For cylindrical molecules of radius *r* and half-height *l*, the following expressions apply to transition moments parallel (||) and perpendicular (⊥) to the cylinder symmetry axis, respectively:

$$G^{\parallel} = \frac{l}{\sqrt{l^2 + r^2}} - \frac{2}{3} \tag{23}$$

$$G^{\perp} = \frac{1}{2}\left[\frac{2}{3} - \frac{l}{\sqrt{l^2 + r^2}}\right] \tag{24}$$

$CuPcS_4$ is a disk-shaped molecule for which $r/l \gg 1$, and the $\pi-\pi^*$ transition moment is perpendicular to the "cylinder axis".[15] Hence, the relevant factor in eq 22 is $G^{\perp}$, which is positive for $r/l \gg 1$. Generally speaking, the (frequency-dependent) dielectric constant and refractive index of the solvent will increase upon the addition of salt, which according to eq 22 should lead to a reduction in the oscillator strength of the molecule, in agreement with our experimental results. It should be noted that any interactions involving permanent electric dipoles on the solute or the solvent are ignored in the theory, but experimental results presented in ref 14 indicate that these interactions do not alter the general trends predicted by eq 22.

In summary, model UA1 provides excellent fits to the experimental results over the full range of dye and salt concentrations considered. The MD model provides a poor fit to the experimental results for the pure-water solution but improves as salt is added. The equilibrium constants obtained by fitting model UA1 indicate a decrease in aggregation with increasing salt concentration, whereas the MD results show an increase in aggregation. It is notable that the fitted values of the parameter υ_{ex} from model UA2 are at variance with those from models UA1 and MD despite the curves for UA2 and MD being almost indistinguishable. This is due to the constraint that all equilibrium constants are equal (i.e., $\upsilon_{ex} = \upsilon_{in}$), probably leading to an underestimation of the dimer concentration and an overestimation of the higher-aggregate concentrations.

5. Conclusions

In this paper, we have investigated the aggregation properties of $CuPcS_4$ in aqueous salt solutions using UV−vis spectroscopy and equilibrium statistical mechanics. By exploiting the sensitivity of the peak intensities at the absorption maxima, we have been able to extract the $CuPcS_4$ concentration dependence of the equilibrium cluster distribution. We have shown that the monomer−dimer model (MD) is unable to describe the qualitative behavior of the molar absorption coefficients at $CuPcS_4$ concentrations above 10^{-4} M. We have put forward an alternative model (UA1) that takes into account the formation of trimers and all higher aggregates. It has been demonstrated that the new model provides excellent fits to the experimental results over the entire range of $CuPcS_4$ concentrations considered. A third model (UA2) has also been examined, which describes the formation of trimers and higher aggregates according to an equilibrium constant equal to that for the monomer−dimer equilibrium. In each case considered in this work, model UA2 produces a fit indistinguishable from that provided by the simple monomer−dimer equilibrium, albeit with different fit parameters.

We have also investigated the variation of the equilibrium constants with increasing salt concentration. This is of practical concern in the dye industry because the dyeing process is carried out in the presence of salt and the optical properties of the dye are clearly sensitive to the degree of aggregation. The effects of ionic strength may also be significant in the aggregation of Pcs in intracellular media; this is of great relevance to photodynamic therapy. A typical cellular environment may have an ionic strength of ∼0.1 M, which we have shown is high enough to affect strongly the aggregation of Pc molecules. It appears that the choice of model is crucial when assessing the degree of aggregation in the presence of added salt. In previous studies,[4,6,10] it was claimed that aggregation is enhanced upon the addition of salt. We have confirmed for $CuPcS_4$ in aqueous NaCl solutions that a naïve analysis using the monomer−dimer equilibrium does indeed lead to this conclusion. The rationale traditionally put forward is that the ionic screening provided by the salt reduces the repulsions between like charges on the solute molecules. This is unlikely because even in a typical room-temperature aqueous solution of a univalent electrolyte with an ionic strength of, say, 0.1 M, the Debye−Hückel estimate of the screening length is around 3 nm (i.e., at least as large as molecular dimensions). At lower salt concentrations, the screening length will be even longer, and hence the short-range behavior of the interaction potential responsible for aggregation should be quite insensitive to the ionic strength. This is in contrast to colloidal dispersions in which the "solute" colloid particles have diameters on the order of 10^{-6} m; in this case, the solute size is at least as large as typical screening lengths.

As mentioned above, model UA1 proposed in this work is quantitatively more reliable than models UA2 and MD. Equilibrium constants obtained with model UA1 indicate that

aggregation is suppressed when the salt concentration is raised above 0.01 M. One possible explanation is as follows. Regardless of the salt concentration, the formation of clusters from an initial pure-monomer state is accompanied by a decrease in $\pi-\pi$ interaction energy, $\Delta U_{\pi\pi} < 0$, and a decrease in entropy, $\Delta S < 0$, because of the confinement within each cluster. The total Gibbs free energy change is then $\Delta G \simeq \Delta U_{\pi\pi} - T\Delta S$ (ignoring the $P\Delta V$ term, which is likely to be insignificant). In the presence of salt, there will be an additional contribution to the interaction energy from Coulombic interactions between solute and electrolyte, U_C. The Coulombic energy contribution (per molecule) should be more negative for free molecules than for aggregated molecules because in the latter case the solvent and electrolyte would be excluded from the region of each solute−solute "bond". Hence, $\Delta U_C > 0$, and so the total Gibbs free energy change, $\Delta G \simeq \Delta U_{\pi\pi} + \Delta U_C - T\Delta S$, will increase with increasing salt concentration, leading to an overall reduction in the degree of aggregation. In effect, the addition of salt might energetically stabilize free molecules with respect to the aggregates. It is also likely that solute−solvent and solvent−solvent interactions play an important role in stabilizing or destabilizing aggregates.[16]

Finally, we have observed that the fitted molar absorption coefficients for monomers, external molecules, and internal molecules all decrease with increasing salt concentration, regardless of the model used. We have confirmed that this trend is in agreement with the theoretical predictions of Myers and Birge,[14] which correlate changes in the oscillator strength with the molecular geometry and the refractive index of the solvent.

Acknowledgment. This research was supported by the Engineering and Physical Sciences Research Council through studentships to R.K.N. and N.M.S. We thank Warren Ebenezer and Mike Hutchings of DyStar UK Ltd. for making us aware of the significance of aggregation in the dyestuffs industry.

Appendix A: Solution of the Cubic Equation

The solution of eq 10 to yield the monomer fraction, x_1, is obtained as follows (see, for example, ref 17). First, rewrite it in the form

$$z^3 + a_2 z^2 + a_1 z + a_0 = 0 \tag{25}$$

where z is written in place of x_1 and the coefficients are given by

$$a_2 = \frac{2\upsilon_{ex}c - 2\upsilon_{in}c - (\upsilon_{in}c)^2}{(\upsilon_{in}c)^2 - \upsilon_{ex}\upsilon_{in}c^2} \tag{26}$$

$$a_1 = \frac{1 + 2\upsilon_{in}c}{(\upsilon_{in}c)^2 - \upsilon_{ex}\upsilon_{in}c^2} \tag{27}$$

$$a_0 = \frac{-1}{(\upsilon_{in}c)^2 - \upsilon_{ex}\upsilon_{in}c^2} \tag{28}$$

Define the following combinations:

$$Q = \frac{3a_1 - a_2^2}{9} \tag{29}$$

$$R = \frac{9a_1a_2 - 27a_0 - 2a_2^3}{54} \tag{30}$$

$$D = Q^3 + R^2 \tag{31}$$

With typical values of υ_{ex}, υ_{in}, and c, $D < 0$, which implies that all three solutions of eq 25 are real. Defining the quantity

$$\theta = \arccos\left(\frac{R}{\sqrt{-Q^3}}\right) \tag{32}$$

the solutions of eq 25 are given by

$$z_1 = 2\sqrt{-Q}\cos\left(\frac{\theta}{3}\right) - \frac{1}{3}a_2 \tag{33}$$

$$z_2 = 2\sqrt{-Q}\cos\left(\frac{\theta + 2\pi}{3}\right) - \frac{1}{3}a_2 \tag{34}$$

$$z_3 = 2\sqrt{-Q}\cos\left(\frac{\theta + 4\pi}{3}\right) - \frac{1}{3}a_2 \tag{35}$$

With physically relevant parameters, the required solution of eq 10 is $x_1 = z_3$.

References and Notes

(1) *Phthalocyanines: Properties and Applications*; Leznoff, C. C., Lever, A. B. P., Eds.; VCH: New York, 1989.
(2) Kasha, M.; Rawls, H. R.; El-Bayoumi, M. S. *Pure Appl. Chem.* **1965**, *11*, 371.
(3) Schutte, W. J.; Sluyters-Rehbach, M.; Sluyters, J. H. *J. Phys. Chem.* **1993**, *97*, 6069.
(4) Gruen, L. C. *Aust. J. Chem.* **1972**, *25*, 1661.
(5) Yang, Y.-C.; Ward, J. R.; Seiders, R. P. *Inorg. Chem.* **1985**, *24*, 1765.
(6) Martin, P. C.; Gouterman, M.; Pepich, B. V.; Renzoni, G. E.; Schindele, D. C. *Inorg. Chem.* **1991**, *30*, 3305.
(7) Piechocki, C.; Simon, J.; Skoulios, A.; Guillon, D.; Weber, P. *J. Am. Chem. Soc.* **1982**, *104*, 5425.
(8) Mausurel, D.; Sirlin, C.; Simon, J. *New J. Chem.* **1987**, *11*, 455.
(9) Schouten, P. G.; van der Pol, J. F.; Zwikker, J. W.; Drenth, W.; Picken, S. J. *Mol. Cryst. Liq. Cryst.* **1991**, *195*, 291.
(10) Neumann, B. *Langmuir* **2001**, *17*, 2675.
(11) Neumann, B.; Huber, K.; Pollmann, P. *Phys. Chem. Chem. Phys.* **2000**, *2*, 3687.
(12) van Roij, R. *Phys. Rev. Lett.* **1996**, *76*, 3348.
(13) van Roij, R. Simple Theories of Complex Fluids. Thesis, University of Utrecht, Utrecht, The Netherlands, 1996.
(14) Myers, A. B.; Birge, R. R. *J. Chem. Phys.* **1980**, *73*, 5314.
(15) Stillman, M. J.; Nyokong, T. In *Phthalocyanines: Properties and Applications*; Leznoff, C. C., Lever, A. B. P., Eds.; VCH: New York, 1989; Chapter 3, p 133.
(16) van der Pol, J. F.; Neeleman, E.; Zwikker, J. W.; Nolte, R. J. M.; Drenth, W.; Aerts, J.; Visser, R.; Picken, S. J. *Liq. Cryst.* **1989**, *6*, 577.
(17) Abramowitz, M.; Stegun, I. A. *Handbook of Mathematical Functions*; Dover Publications: New York, 1965.